N87-11193

EFFECTS OF SURFACE CHEMISTRY ON HOT CORROSION LIFE*

R. E. Fryxell

General Electric Company
and
B. K. Gupta

TRW, Inc.

This program has as its primary objective the development of hot corrosion life prediction methodology based on a combination of laboratory test data and evaluation of field service turbine components which show evidence of hot corrosion. This program is divided into five tasks. Burner rig testing is being performed by TRW. The discussion will describe the overall program with a summary of results obtained in the first two tasks which have been completed.

Task I involves a comprehensive evaluation of six hot corroded turbine components, having known operating history, to establish the degradation mechanisms in the corroded areas. The six components selected are identified in Table I. Four of these are the same component from engines of the same model to afford maximum opportunity to make cause and effect correlations. The high pressure turbine (HPT) components were obtained only after examining blades from a large number of disassembled engines; hot corrosion is only infrequently substantial in the HPT of engine models available for this study. On the other hand, hot corrosion is more frequently encountered in the low pressure turbine (LPT) since at the lower temperatures involved, corrosive contaminants are more likely to accumulate in significant amounts and/or be present a greater percentage of operating time. One LPT vane is included in this study for comparison.

Evaluation of these components included optical metallography, scanning electron microscopy (SEM), and electron microprobe (EMP) examination. Several transverse sections of each airfoil were prepared using nonaqueous cutting and polishing techniques.

PRECEDING PAGE BLANK NOT FILMED

* Contract NAS3-23926

Results of the evaluation of the four CF6-50 Stage 1 blades are summarized in Table II. Locations at which maximum degradation was observed in individual sections are defined by % span (radial)/% chord (distance from leading edge (LE) to trailing edge). These observations are limited to the leading edge and concave/pressure surface; the convex surface of such blades rarely suffers significant environmental degradation. The listed temperatures refer to the blade surface at the location of maximum degradation; these must be regarded as approximate for two reasons: (1) the observed distress occurs over some distance along the surface, and (2) assigned temperatures are calculated and will, in general, change somewhat as the turbine ages.

Typical sulfidation was noted at some locations in all of these blades, including development of a depletion layer (loss of aluminum) in the coating or substrate alloy. Typical microstructures are shown in Figures 1 and 2. However, sulfides were found in the most distressed areas in only two of these blades. In the other two blades, although sulfides were found, the most severely distressed regions did not contain any detectable sulfides.

This points up a primary difficulty in interpretation, namely that contaminant ingestion occurs only when the aircraft is near ground level; during most of a mission, simple oxidation is probably to be expected. Table II exhibits one attempt to relate the observed degradation to operating history. Using flight pattern information and the criterion given in footnote (a), total times were estimated during which each engine might be considered vulnerable to contaminant ingestion: total hours near coastal airports, and total hours (in life of engine). One way of displaying this information is shown in Figure 3. There is in fact a trend showing increased hot corrosion with increased low altitude operating time; the curvature is upwards as is not unreasonable, i.e., above about 60-80 μm (nominal original coating thickness) the substrate alloy is exposed. However, with this limited sampling, it is not possible to make inferences concerning coastal versus total low altitude exposure.

Alternatively, the trends shown in Figure 3 may reflect total times at takeoff/thrust reverse (higher) temperatures, a parameter which is clearly related to total hours at low altitudes. This is shown in rate units (Figure 4). The highest rates correspond to the shortest lengths of mission for which the percentage of time at higher temperatures (or lower altitude) is greater.

These are in fact interesting and instructive exercises, but remembering that the present four blades were selected as rather extreme examples, the actual amounts of corrosive degradation (Table II and Figures 3 and 4) do not define possible curves which other examples should be expected to match. Further, since oxidation and hot corrosion rates are competitive in some instances (Table II), the cause and effect relationships with respect to environmental degradation have that additional degree of complexity.

The trend shown in Figure 4 has, however, long been recognized in a qualitative sense and hopefully continued quantitative evaluations coupled with compilations of operating histories will lead to a reliable choice between various possible correlations such as those depicted in Figures 3 and 4.

With respect to the ultimate blending of this type of information with the burner rig studies to be performed in this program and application to life prediction methodology, it should be pointed out that previous burner rig corrosion tests at General Electric with very low salt ingestion levels (at barely the threshold level for salt condensation) produced conventional Type 1 sulfidation but at rates indistinguishable from oxidation. This may relate to the results in Table II, namely that oxidation and corrosion rates may vary relative to each other, depending on the circumstances. Possibly as well there are implications with respect to the design of somewhat more complex burner rig tests; i.e., temperature cycling, intermittent salt ingestion, etc.

Evaluation of the other two components listed in Table I revealed extensive Type 1 sulfidation in the low pressure turbine vane but not in the J79 high pressure turbine blade. Since these are different components/different engine models, the observations cannot be factored into an operating history correlation together with the other four components. Yet the structural features of the degradation do contribute to baseline service related information to be compared with hot corrosion burner rig tests which comprise the remainder of this program.

Two of the three burner rig tests are to be conducted under identical conditions as described in Table III for a maximum time of 1000 hours (see Figure 5). The first of these, Task II, provides a hot corrosion baseline for the program alloys and coatings in the as-processed condition. Included in this task are duplicate specimens of U700 and Rene' 80, both uncoated and with the following coatings:

> pack aluminide RT21 (Chromalloy) and Codep (General Electric)
> low pressure plasma NiCoCrAlY (Ni-23Co-18Cr-12Al-0.3Y)

At approximately 20 cycle intervals, specimens are visually examined, photographed, and coil inductance measurements made in a series mode at 10MHz with a multifrequency LCR meter as shown in Figures 6 and 7. These measurements are patterned after studies at NASA-LeRC during the past several years. Specimens are removed from the test when visual evidence of hot corrosion is noted in three successive inspections. Additional specimens are also exposed for lesser time periods. Specimen evaluation is performed as in Task I.

A second identical hot corrosion burner rig test (Task IV) will be performed with specimens which have been given a variety of aging treatments at 1100C (Task III) to determine the effect on hot corrosion behavior caused by surface oxidation and/or interdiffusion between coating and substrate alloy. Triplicate specimens of the above coated alloys will be aged under the following conditions: isothermal inert atmosphere (vacuum) for 100 hours, isothermal air furnace oxidation for 100, 300, 600 hours, one hour air furnace cycles for 100 hours and cyclic burner rig oxidation for 100, 300 and 600 hours. One specimen of each material representing each of these conditions will be metallographically evaluated and the remaining duplicates used in the Task IV hot corrosion burner rig test.

The Task II burner rig test has been completed. Coil inductance measurements are shown in Figure 8 for six uncoated specimens. The four long term specimens were removed at the third inspection interval at which hot corrosion was visually observed. Although Rene' 80 and U700 survived about the same lengths of time, based on this criterion, the coil inductances were widely different, and metallographic measurements indicated a factor of two greater corrosion rate for U700, in accordance with previous experience. Typical microstructures with subsurface sulfides are shown in Figure 9 for one specimen of each alloy.

Coil inductance measurements for coated specimens are shown in Figure 10 with an expanded scale below 200 hours to show clearly the negative changes which appeared at the first inspection, particularly for the aluminide coated specimens. The overall changes are in all cases much smaller than for the uncoated alloys (Figure 8) reflecting the corrosion protection offered by all of the coatings. The four Codep coated specimens are shown in Figure 10 to their time of removal and the greater coil inductance changes suggest a greater corrosion rate; for all of these, coating penetration was confirmed metallographically. The three RT21 coated specimens shown in Figure 10 ran the full term 1000 hours with only minor visual evidence of hot corrosion. However, metallographic evaluation showed essential coating penetration in all three, although clearly less extensive than for the Codep coated specimens. One specimen of RT21 coated Rene' 80 (not shown in Figure 10) was removed at 697 hours and did exhibit coating penetration with additional corrosion of the substrate to about 100 μm depth. All of the NiCoCrAlY coated specimens showed extensive alloy depletion within the coating, occasional pits, but no complete penetration was observed. Typical microstructures are shown in Figure 11.

Subsequent to the completion of Task II, all the aging treatments in Task III have been performed and Task IV is underway. At the conclusion of the Task IV test, all the data generated in Tasks I through IV will be evaluated and an empirical hot corrosion life prediction model based on these data will be proposed. Also, recommendations will be made for other test parameters to be evaluated, and evaluation methodology necessary to permit prediction of hot corrosion life.

Task V will be a hot corrosion high velocity cyclic burner rig test designed to check the validity of the proposed life prediction model. Duplicate specimens of a maximum of four alloys and five coatings will be tested up to a maximum of 1000 hours and evaluated as in Tasks II and IV. The alloys and coatings will be those from this program plus additional alloy-coating systems selected by the NASA Project Manager.

The Task V experiment will be designed to test two aspects of the life prediction model developed in Task IV. The ability of the model to predict hot corrosion life under different rig test conditions than those previously used in Task II and IV will be tested in one portion of the experiment. The second portion of the experiment will test the ability of the model to predict hot corrosion life of new alloys and coatings.

The ability of the model to predict hot corrosion life under different rig test conditions will be evaluated using alloys and coatings previously tested in Task II and Task IV. The hot corrosion tests for this portion of the program will use one or more variations of the test parameters used in Task II, III and IV. Test parameter variations that will be considered include the following:

- A different salt level
- A different test temperature
- Intermittent salt injection
- A different sulfur level in the fuel
- Additional or modified aging cycles

The specific testing parameters will be derived from the results of Task II and Task IV, previous experience in evaluating field service hardware and previous experience in conducting hot corrosion testing under a variety of test conditions.

The ability of the model to predict hot corrosion resistance of new coatings and alloys will be evaluated using alloys and coatings that have not been evaluated previously in Task II and Task IV. The aging cycle will be chosen from the results of Task IV.

Life prediction for both portions of the Task V experiment will be based on the model developed in Task IV as well as extensive experience gained from evaluating field service components and conducting hot corrosion tests. Knowledge of the effect of variations in both engine operating conditions and rig testing conditions will be used in predicting hot corrosion life under different rig test conditions in the first portion of the experiment with the same alloys and coatings tested in Task II and Task IV. With respect to testing of additional alloys and coatings, use will be made of extensive empirical correlations of composition and hot corrosion performance in predicting hot corrosion life.

Table I. Components Selected for Evaluation.

Carrier Base	Aircraft	Component	Total Hours	Number of Cycles	% Takeoffs at Coastal Airports
Southern Asia	A300B	(1)	2,694	1560	67
Northern Africa	A300B	(1)	4,641	2169	77
Southern Africa	A300B	(1)	1,830	1471	50
Western Europe	DC10-30	(1)	2,625	610	46
South America	DC10-30	(2)	15,155	2987	72
U.S. Military	F4	(3)	2,700		

(1) CF6-50 Stage 1 high pressure turbine blade, Codep coated Rene' 80.
(2) CF6-50 Stage 1 low pressure turbine vane, uncoated Rene' 77.
(3) J79 Stage 1 high pressure turbine blade, Codep coated Rene' 80.

Table II. Summary of Metallographic Evaluations and Operating History for Four Stage 1 High Pressure Turbine Blades from CF6-50 Engines.

Carrier Base	Total Hours	No. of Cycles	Hours/Cycle	Hours <2000' El.[(a)] Near Coastal AP	Hours <2000' El.[(a)] Total	Location[(b)]	Temp. °C (Est.) Max.	Temp. °C (Est.) Avg.	Maximum Depth of Attack, μm[(c)] Total	Maximum Depth of Attack, μm[(c)] per 1000 Hours	Type 1 Sulfides
Southern Asia	2694	1560	1.72	350	520	40/70-90	1090	820	100	37	Yes
						60/LE	980	740	50	20	Yes
						60/80	1090	820	200	75	No
Northern Africa	4641	2169	2.14	560	720	50/60-90	1090	820	230	50	Yes
						80/50-80	1090	820	230	50	Yes
Southern Africa	1830	1471	1.24	240	490	10/LE	910	680	50	27	Yes
						10/60-80	1020	760	75	40	Yes
						60/90	1090	820	180	100	No
Western Europe	2625	610	4.30	95	200	10/60-80	1020	760	45	17	No
						20/60-80	1020	760	50	20	Yes

(a) Estimated, using 20 minutes as approximate total time per cycle; gate to takeoff, climb to 2000 ft.

(b) % Span/% Chord.

(c) Including depletion zone.

Table III Burner Rig Operating Conditions.

Specimen Temperature - 900° C ± 9° C

Test Cycle - 1 hour at temperature followed by 6 minutes of forced air cooling

Sodium Concentration - 0.5 ppm sodium (±10%) in the combustion gases introduced as aqueous NaCl

Combustion Air Preheat Temperature - 232° C ± 10° C

Specimens - Eight positioned equally on a 4.2 cm (1.64 inch) diameter circle of a holder rotating at 600 rpm

Burner Nozzle Throat Diameter - 2.54 cm (1.0 inch)

Burner Pressure - 1.0 psig

Nozzle Throat to Nearest Specimen - 4.45 cm (1.75 inch)

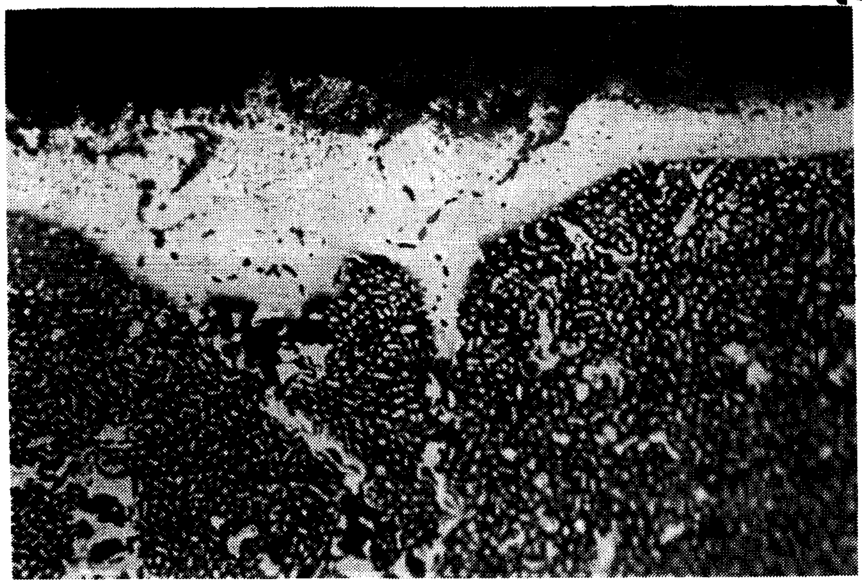

Figure 1. Photomicrograph on the concave airfoil of a Stage 1 high pressure turbine blade from a Northern Africa CF6-50 engine. Sulfides are present in the Rene' 80 depletion zone. Etched, 500X.

Figure 2. Photomicrograph at the leading edge on an airfoil of a Stage 1 high pressure turbine blade from a Southern Africa CF6-50 engine. Sulfides are present within residual coating (arrows). As-polished, 500X.

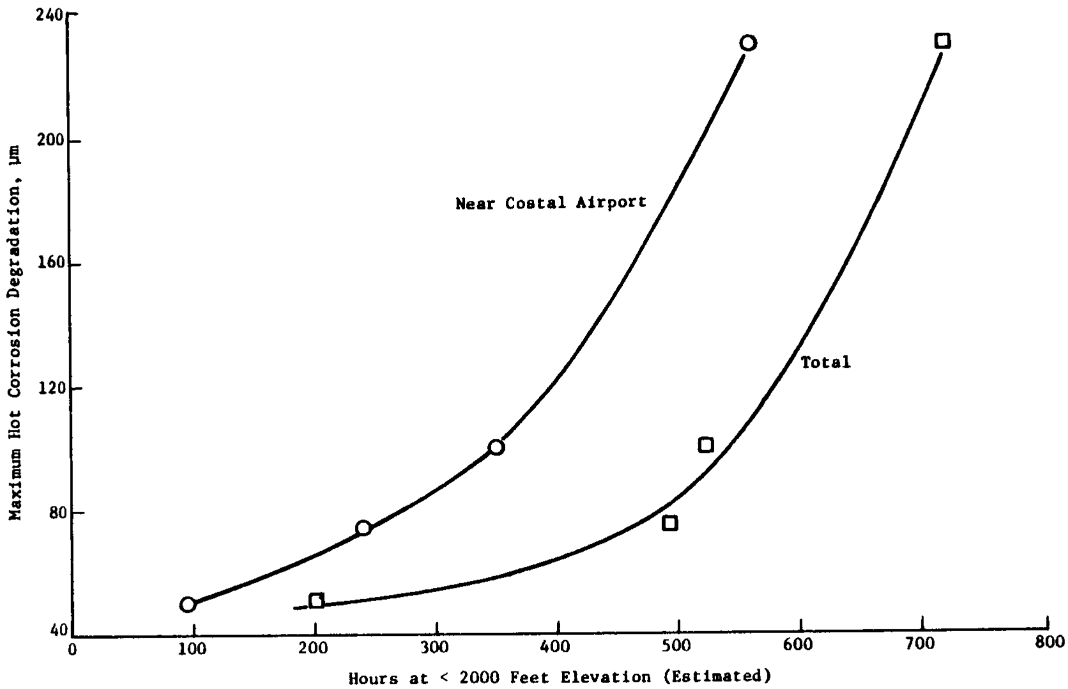

Figure 3. Hot Corrosion Degradation for CF6-50 Stage 1 High Pressure Turbine Blades as Function of Time at Less Than 2000 Feet Elevation.

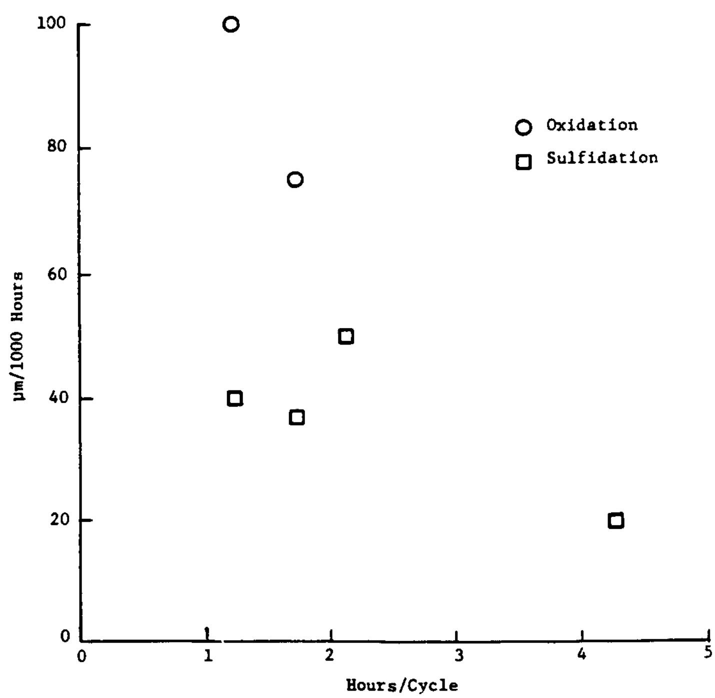

Figure 4. Maximum Degradation Rates for CF6-50 Stage 1 High Pressure Turbine Blades as Function of Average Mission Duration.

ORIGINAL PAGE IS
OF POOR QUALITY

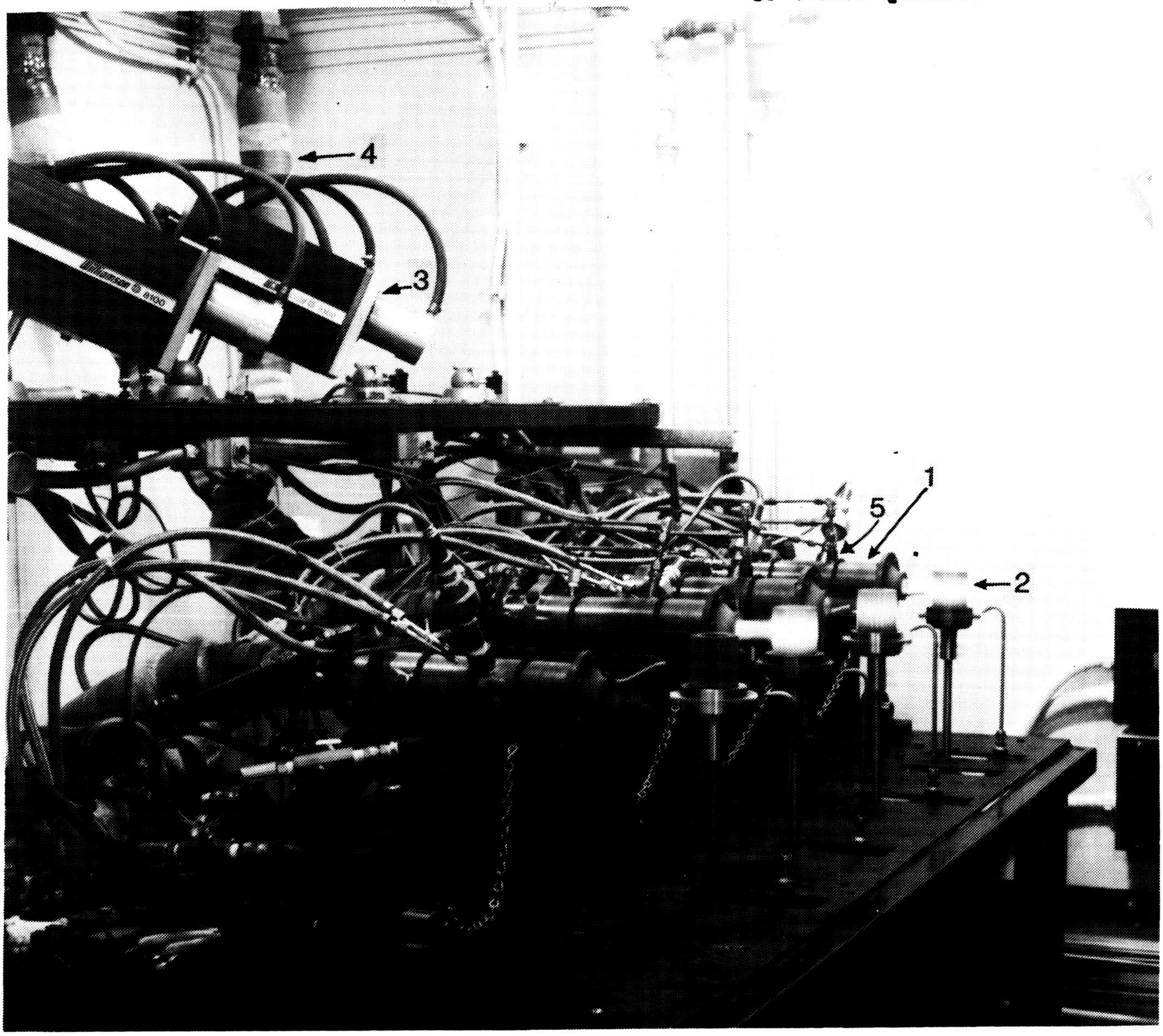

Figure 5. Burner Rigs.

1. Burner
2. Specimens on holder rotating at 600 rpm.
3. Optical pyrometer
4. Preheated combustion air
5. Salt solution spray nozzle

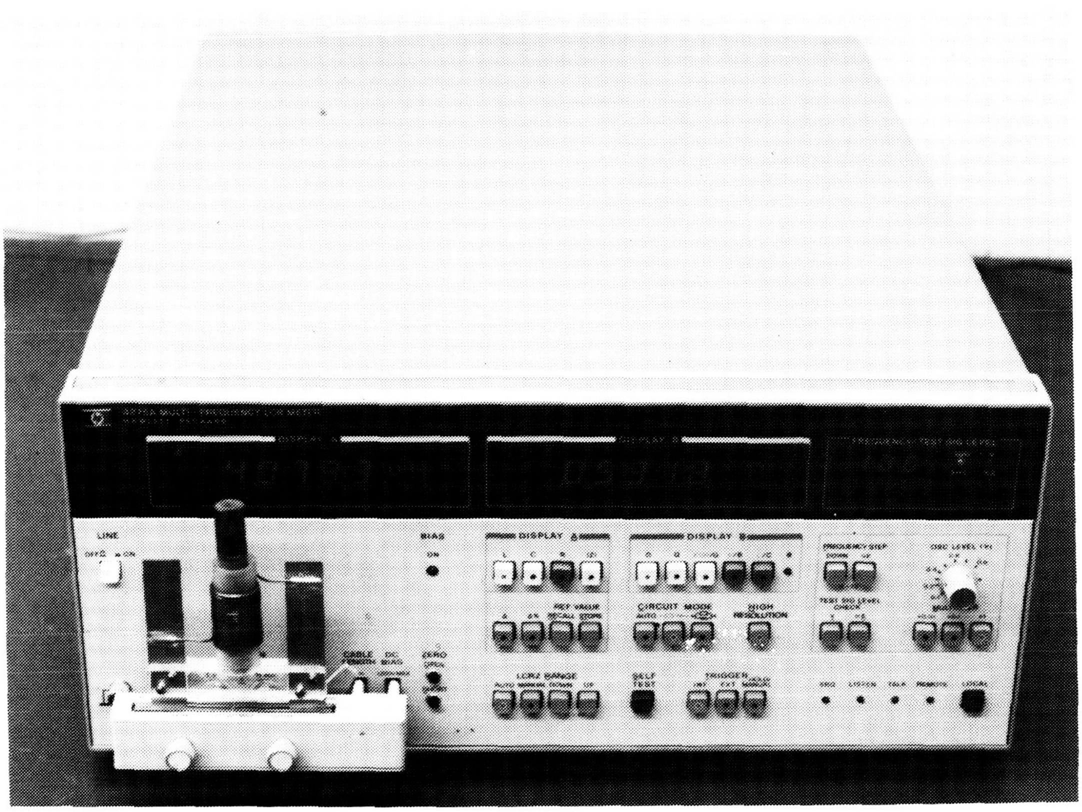

Figure 6. Inductance rig/coil with specimen core.

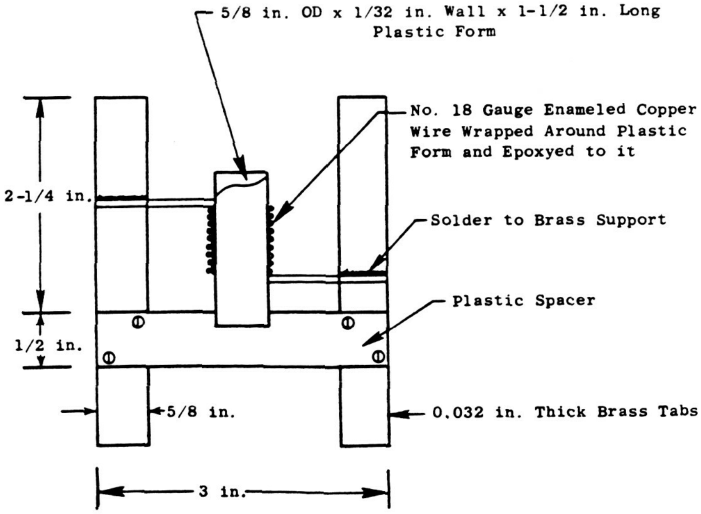

Figure 7. Inductance Coil and Support.

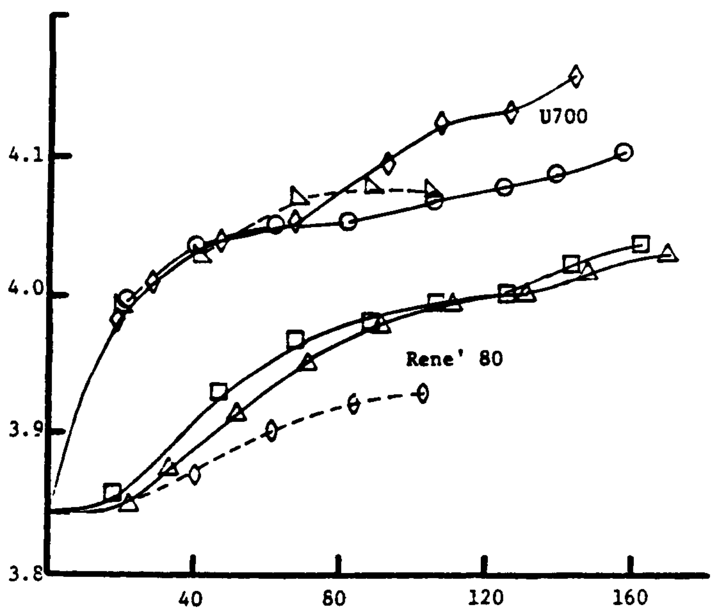

Figure 8. Uncoated Alloy Coil Inductance Changes with Hot Corrosion at 900° C, Cyclic Exposure.

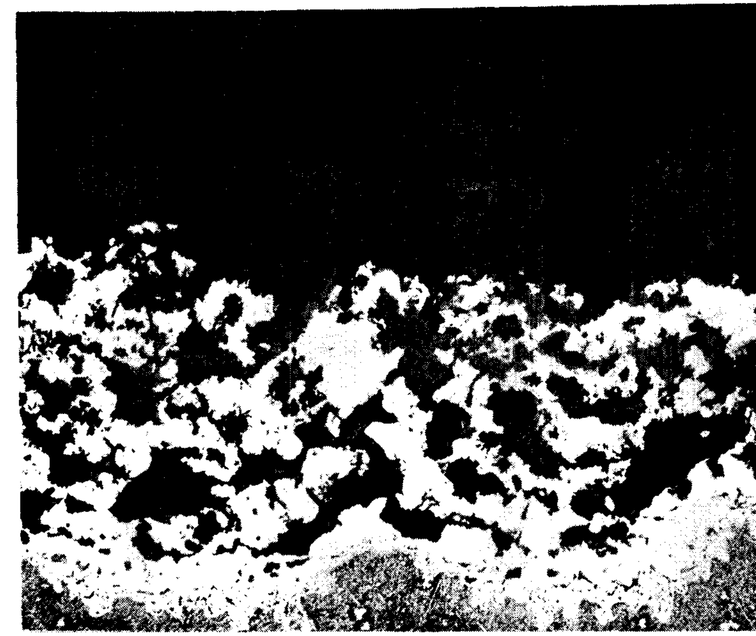

U700, 142.65 hours.

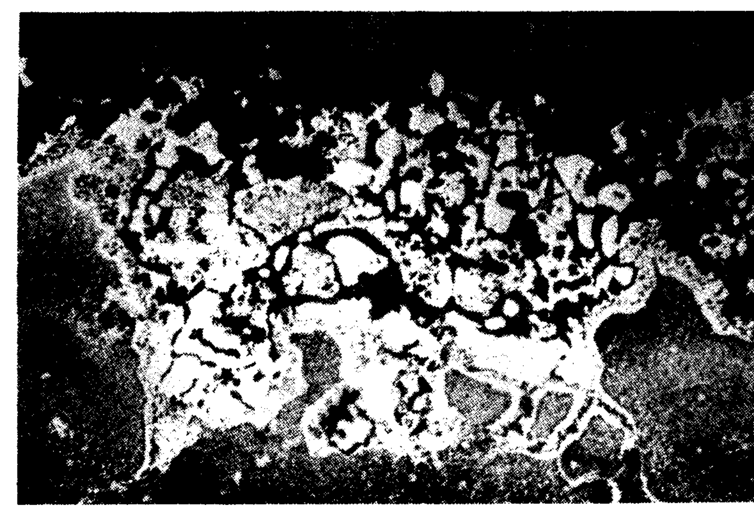

Rene' 80, 167.7 hours

Figure 9. Photomicrographs of specimens from burner rig hot corrosion test. Type 1 sulfides are present. Etched, 200X.

ORIGINAL PAGE IS OF POOR QUALITY

ORIGINAL PAGE IS
OF POOR QUALITY

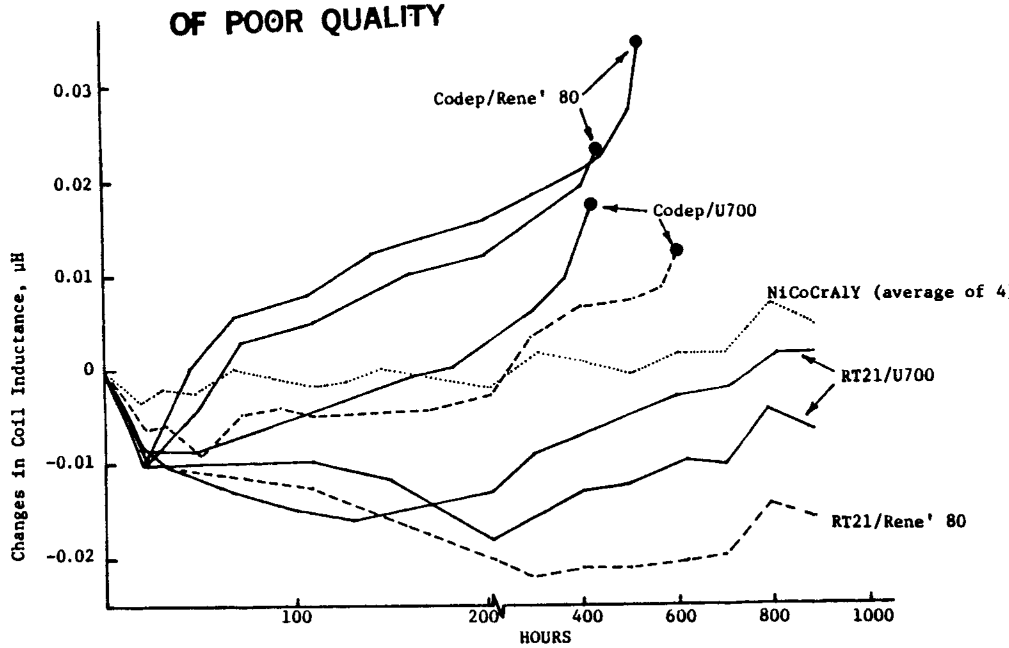

Figure 10. Changes in Coil Inductance with Hot Corrosion at 900C, Cyclic Exposure.

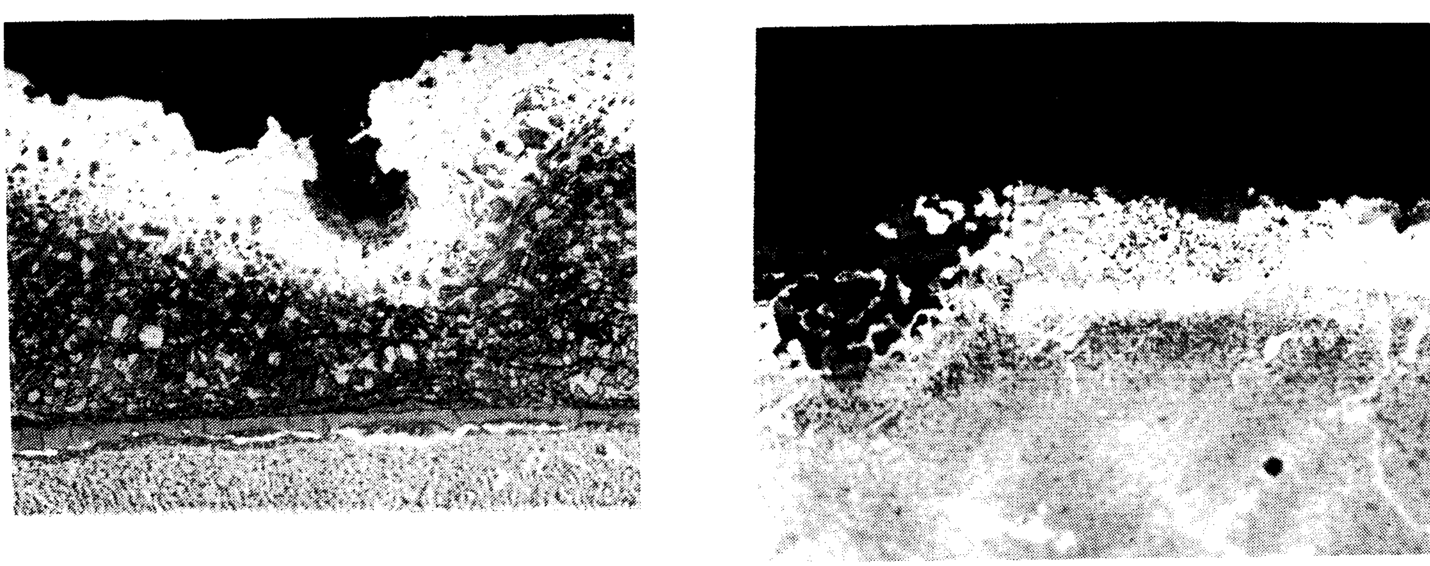

(a) (b)

Figure 11. Photomicrographs of specimens from burner rig hot corrosion test. Type 1 sulfides are present. Etched.

(a) NiCoCrAlY coated U700, 1004.6 hours (500X)
(b) RT21 coated Rene' 80, 697.1 hours (200X)